

# EFFECT OF TIG WELDING PARAMETERS ON WELD POOL DILUTION: A CASE STUDY IN AA 6061 ALLOY

Preethi K. H.<sup>1</sup>, Pradeep H.<sup>2</sup>, Deepika M S.<sup>3</sup>, Dharnish J.<sup>4</sup>, Mahesh G Emmi.<sup>5</sup>

<sup>1</sup>Department of Industrial Engg & Management, Bangalore Institute of Technology, Bangalore-560 004

<sup>2</sup>Dept. Of Mechanical Engg, BGSIT, Mandya Dist-571 448

<sup>3</sup> Dept. Of IEM, Bangalore Institute of Technology, Bangalore-560 004

<sup>4</sup> Department of Mechanical Engg National Institute of Engineering, Mysuru – 57008

<sup>5</sup>Faculty of Management Studies & Advanced Technologies, Airforce Technical College, Bangalore – 560015

**Abstract:** Activating silicon alloy was investigated in tungsten inert gas welding of Al 6061. The results indicated that deep penetrations with different percentages of silicon dilution is due to reverse marangoni flow in the weld bead. It was shown that the Silicon particles were distributed and dispersed in the weld bead and particle content was higher in the center of the weld than at the edges of the weld by the results of SEM and EDS. Fusion zone composition over the full range of dilution levels (0 to 100 pct) were produced by varying the independent welding parameters of current. The mechanical properties of the weld beads were obviously improved by tensile tests and micro hardness tests because of silicon. The results presented from this study provide guidelines for controlling the weld – metal compositions in these fusion-zone combinations.

**Keywords:** Tungsten Inert Gas (TIG) Welding, porosity, Aluminium alloy, Microstructure

## 1. Introduction

Al-Mg-Si alloys are extensively used in defence and aerospace applications. Tungsten inert gas (TIG) welding is an arc welding process that produces coalescence of metals by heating them with an arc between a non-consumable electrode and the base metal. The TIG welding process [1] is generally used for welding of these alloys. The various techniques in the TIG welding process are pulsing and magnetic arc oscillation. By using the materials in solution, heat-treated and artificial ageing condition the complete weld, heat-affected zone, and parent metal can be aged in a single post weld heat treatment. However, difficulties have been reported in obtaining satisfactory properties in as-welded condition particularly strength and toughness due to low dilution of the base metal into the weld [2]. There are various methods such as inoculation with heterogeneous nucleates, surface nucleation, and dilution to improve the grain refinement in the weld zone. The use of inoculation for refining the fusion zone is successful in casting but not in welding [3]. Surface nucleation technique was also not much popular because of the complicated setups and procedures associated with its use.

The purpose of the present investigation is to improve the dilution of the base metal into the weld in pulsed TIG welding process. Metallurgical advantages of pulsed current that are frequently reported in the literature include grain refinement in the fusion zone, reduced width of heat-affected zone (HAZ), less distortion, control of segregation, reduced hot cracking sensitivity, and reduced residual stresses [4, 5]. Grain refinement reduces hot cracking sensitivity in heat-treatable alloys by using pulsing and magnetic arc oscillation [6]. Dilution of the base metal into the fusion zone that provides sufficient amount of grain refinement is more effective than the filler metal containing refining elements [7, 8]. Hence dilution is more important in heat-treatable alloys because it reduces hot cracking sensitivity and improves mechanical properties.

## 2. Dilution

Variation of weld geometry with respect to amount of weld deposition and fusion of base metal affects the weld bead dilution defined as a ratio of the (amount of the fused base metal/ total amount of molten weld metal). They are generally estimated by measuring area of used region of base plate and total area of weld as revealed in transverse section of bead on plate weld deposit. The dilution of weld especially in case of using dissimilar filler wire significantly affects its chemical and metallurgical properties. Thus in case of variation in weld geometry it is imperative to study the dilution of weld metal. In the line of general understanding on weld geometry affecting the dilution, here also the increase of  $\beta$  from 0.05 to 0.1 relatively enhances the dilution followed by a considerable reduction in it with a further increase of  $\beta$  up to 0.3 or 0.4 at a given conventional energy input and mean current. At a given  $\beta$  and mean current the increase of energy input and at a given  $\beta$  and energy input the increase of mean current enhances the dilution of weld bead primarily due to increased heat and heat build-up in the weld pool causing larger melting of base metal. Further due to comparatively larger melting of base plate, the Al-Mg alloy [15] undergoes through relatively larger dilution of weld deposit than aluminum especially at higher mean current. But, the dilution being a function of several interactive aspects of weld geometry its correlation with any individual pulse parameter except mean current is not very conclusive due to significant scattering as it is reported [15] in case of bead on plate deposition on Al-Mg-Zn alloy. However, while considering the summarized effect of pulse parameters, increase of  $\beta$  clearly shows linear reduction of dilution ( $D_n$ ) and penetration ( $P_n$ ) but at a comparatively slower rate at lower mean current. The correlation of hardness and welding dilution with the abrasive mass loss of samples welded with

different welding currents and polarities was studied [16]. A mathematical model simulating the effects of surface tension (Marangoni effect) on weld pool fluid flow and weld penetration in spot gas metal arc welding (GMAW) was studied. [17].

**3. Experimental procedure**

Bead-on-plate welds were produced using the gas tungsten-arc welding (GTAW) process by directly feeding the filler metal into the weld pool of the substrate (figure1). With the non-consumable-electrode GTAW process, the volumetric filler-metal feed rate (V<sub>fm</sub>) and arc power (VI) can be independently controlled, thus easily changing the dilution levels.

The base material employed in this study is 3mm-thick Al-Mg-Si aluminum alloy welded with 4043 filler material. The EDS chemical composition of the base material at Top, middle, bottom weld portion and filler material are shown in Table 1&2. The selection of the filler material is based on the mechanical properties and resistance to cracking in the weld [9].

Table 1:EDS Chemical composition of the base material and filler material (wt.%)

Element Al 6061	Mg	Si	Ti	Cr	Mn	Fe	Cu	Zn	Al
TOP	1.56	1.02	0.28	0.32	0.18	1.48	0.39	0.31	Bal.
MIDDLE	1.54	0.86	0.3	0.44	0.3	0.41	0.58	0.34	Bal.
BOTTOM	0.91	0.91	0.19	0.17	0.21	0.55	0.46	0.36	Bal.

Table 2:EDS Chemical composition of the filler material (wt.%)

Element	O	Mg	Al	Si	Ti	Cr	Mn	Fe	Cu	Zn
Filler alloy Wt. % 4043	1.01	0.61	90.81	5.09	0.41	0.04	0.45	0.5	0.58	0.53

Plates of AA6061 aluminium alloy were machined to the required dimensions (50 mm × 50 mm × 3 mm) and welded with the help of electrode and filler alloy. Proper edge preparation is done to achieve good joints. Double V butt joint configuration was prepared to fabricate TIG welded joints. All necessary care was taken to avoid joint distortion. A graded filler alloy of ER4043 was used with the following particulars: Thickness (T) = 3 mm, Root gap (G) = 2 mm, Root face (R) = 2 mm, and Bevel angle (V) = 45°. The welding has been carried out in a AC/DC TIG ARC 315P DMM machine with varying current from 70, 75, 80, 85, 90 Amp. Table 3. Shows the Standard welding parameters. Diameter of the filler rod is 2.4mm, and length is 1m.

Table 3: Welding parameters

Parameters	Value
Electrode type	DCEN, W-2% ThO <sub>2</sub>
Diameter of the Electrode	2.4mm
Vertex angle of the electrode	60°
Shield gas and flow rate	Ar, 15L/min
Welding current	70-90Amps
Welding speed	2mm/sec

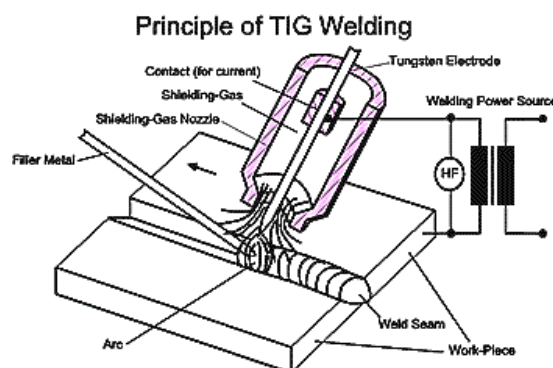


Fig.1: Schematic view of the TIG process for similar joint of Al alloy

Weld metal dilution is as follows [6, 8]. In the fully mixed fusion zone, the final weld composition will simply be a mixture of the substrate and filler metal: In the fully mixed fusion zone, the final weld composition will simply be a mixture of the substrate and filler metal:

$$C_{fz} = C_{fm} (1-D) + C_s(D) \tag{1}$$

Where C<sub>fz</sub>, C<sub>fm</sub> and C<sub>s</sub> are the elemental composition of the fusion zone, filler metal and substrate respectively and D is the dilution level. Thus, when C<sub>fz</sub>, C<sub>fm</sub> and C<sub>s</sub> are all known, the dilution level is simply determined by

$$D = (C_{fz} - C_{fm}) / (C_s - C_{fm}) \tag{2}$$

The values for the major constituents of Al and Si were used to get the final dilution level at Top, middle and bottom of weld portion in TIG. Dilution levels were also determined using metallographic methods to measure the individual geometric cross-sectional

areas of the deposited filler metal and melted substrate. The ratio of the melted substrate ( $A_s$ ) to the total melted cross sectional area from the filler metal and substrate ( $A_s+A_{fm}$ ) is the dilution level (Figure. 2):

$$D = A_s / (A_s + A_{fm}) \quad [3]$$

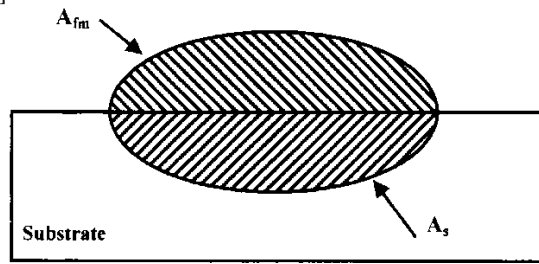


Fig. 2: Schematic illustration of the geometric measurements made for the dilution calculations using Eq. [3].

**4. Results and Discussion**

**4.1 Dilution levels of Al, Mg and Si at Top, Middle and Bottom fusion welds**

Samples are used to obtain a wide range of dilution levels at top, middle and bottom fusion welds between Al6061 and Filler 4043. Filler –metal feed speeds between 2mm/s were used, while the current (I) was varied between 70A and 90 A in 5 A increments.

**Table 4: Dilution level of Aluminium**

SL. NO.	I in Amperes	D(%)-TOP	D(%)-Middle	D(%)-Bottom
1	70	11.81	57.1	14.4
2	75	15.44	46.46	36.46
3	80	10.25	43.6	37.89
4	85	16.09	46.85	42.31
5	90	15.44	48.28	46.46

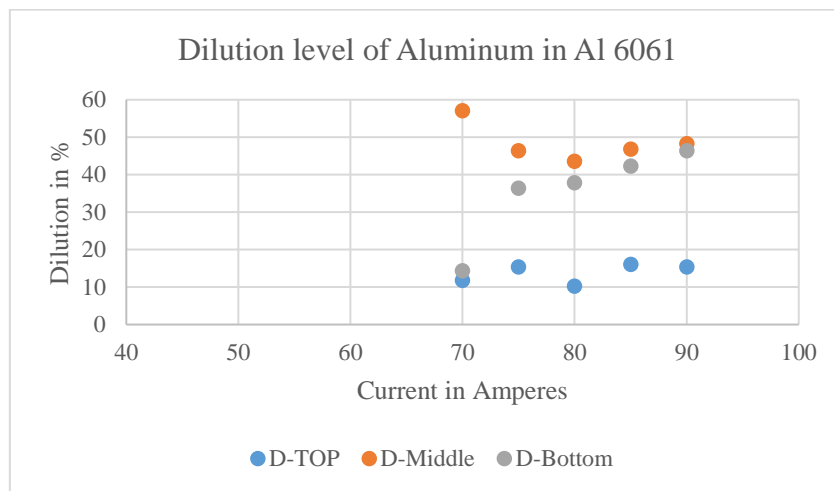


**Fig.3 Dilution level of Aluminium**

Following observations were made for the Aluminium A16061 with 4043 as filler alloy by varying the current.

Figure 3 Shows variation of dilution at top, middle and bottom in percentage with respect to current. It is seen from the figure that the dilution level at the bottom increases with increase in current. The lowest value of dilution 10.25% is observed at current 80A, whereas maximum value of 16.09% is observed at current 85A for dilution at top.

Looking at the dilution level in the middle, dilution level decreases with increase in current up to 80A further increase in current increase in the value of dilution is observed with highest value of 57.1% at lower value of 70A and lowest value of 43.6% at current value of 80A.

Comparing the dilution level at top, middle and bottom for a particular current it is seen that the dilution level at bottom is greater than dilution level at top and dilution level at middle is greater than bottom. It is seen that for all the current value the dilution level is less than 20% at top, 40-60% for middle and less than 50% at bottom.

**Table 5:** Dilution level of Magnesium

SL.NO.	I in Amperes	D(%)-TOP	D(%)-MIDDLE	D(%)-BOTTOM
1	70	15.78	96.77	2.24
2	75	63.15	91.39	13.48
3	80	15.78	98.92	16.85
4	85	29.47	88.1	37.07
5	90	36.84	95.69	51.68

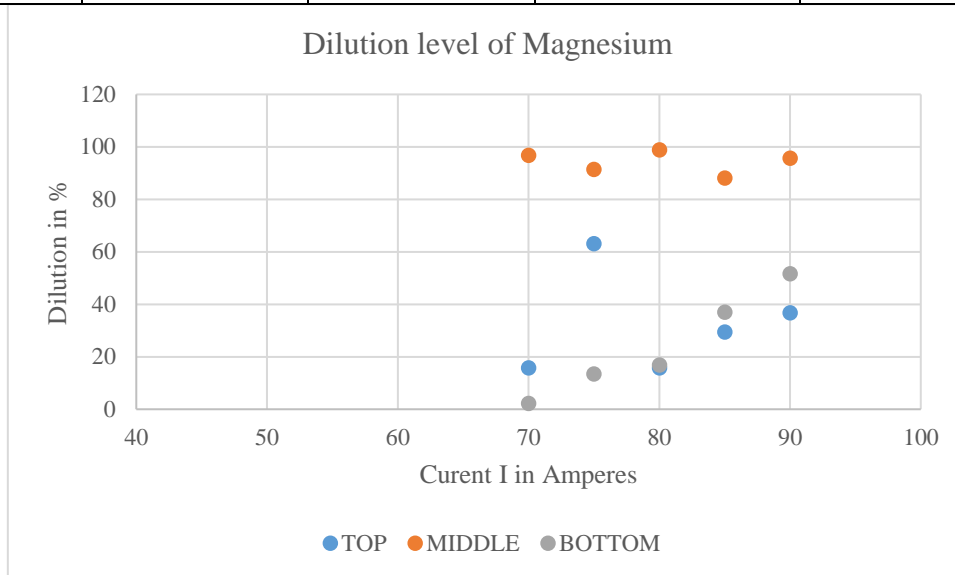


**Fig. 4:** Dilution level of Magnesium

The Variation of dilution at top, middle and bottom with respect to current is shown in fig.4. Considering the dilution at bottom it is observed that the dilution increases with increase in current with the lowest value of 2.24% for the current value of 70A and a maximum of 51.68% at current value of 90A. It is also observed that up to a current value of 80A, the increase in dilution value is less, whereas beyond 80A the dilution level is almost double.

It is seen that there is no systematic variation in dilution with respect to increase in current is observed. Only little variation in dilution with respect to current is observed i.e., the value ranges from 88.1% at current value of 85A and maximum value of 98.92% for current value 80A is seen.

Referring to fig.4 except at current value 75A showing highest dilution value of 63.15% but at other current values the dilution value ranges from 15.78% to 36.84% for the current values 70A and 90A respectively.

Comparing the dilution between top, middle and bottom, for the first two current values (70A & 75A), the dilution level at top is greater than dilution level at the bottom and less than the dilution of the middle for the remaining current values (80, 85 & 90A). The dilution level at the bottom are greater than the dilution level of top but less than the dilution level of the middle.

In over all the dilution level at the top is less than 65%, bottom it is less than 55% and in the middle it varies from 88 to 99%. Also uniformity in dilution level is observed in the middle portion.

**Table 6:** Dilution level of Silicon

SL.NO.	I in Amperes	D(%)-TOP	D(%)-Middle	D(%)-Bottom
1	70	3.17	99.54	8.847
2	75	82.76	95.69	33.33
3	80	39.90	97.05	24.94
4	85	19.50	93.19	56.01
5	90	59.63	97.27	62.35

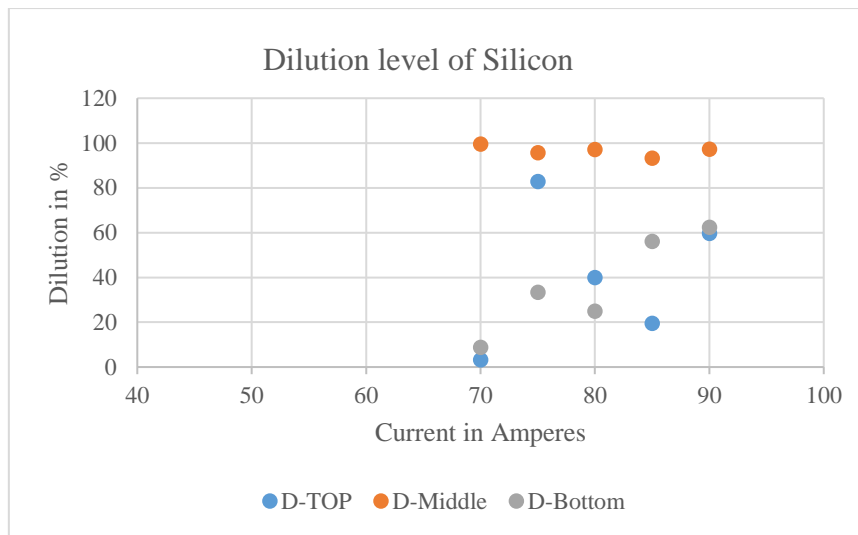


**Fig. 5:** Dilution level of Silicon

Figure 5 Shows the variation of dilution at top, middle and bottom with respect to increase in current for the element silicon. Referring to the dilution at top,middle and bottom there is no systematic variation with increase in current observed.Considering dilution at top, the dilution is good for the current value of 75 and 90A with dilution value of 82.76% and 59.63% respectively. It is seen that dilution at bottom for the first two currents(70 &75A) dilution increases but there is a decrease in value observed at 80A, further increase in current the dilution increases with a maximum of 62.35% observed at current value of 90A. Not much variation in dilution is observed for the middle i.e., with a lowest value of 93.19% at 85A and highest value of 99.54% for current 70A. Whereassimilar value of dilution of around 97% is observed for the currents 80 &90. In over all the current value 90A shows good dilution at top, middle and bottom. Comparing between dilution at top,middle and bottom middle level dilution shows consistent value for all the currents applied and the value ranges from 93 to 99%.

**4.2 Correlation of Hardness and Dilution levels**

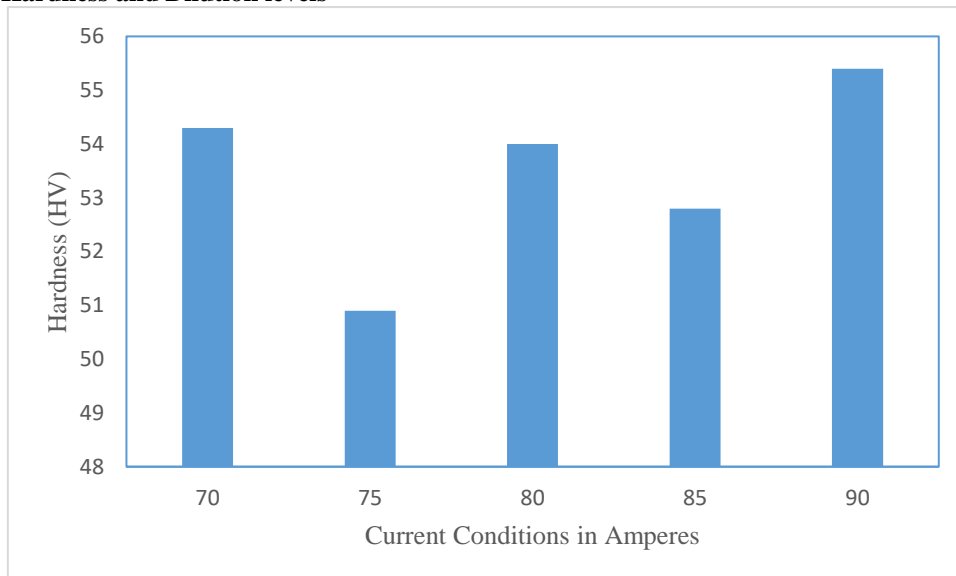


**Fig.6:** Average hardness values at different current condition

Hardness test was done by using Vickers hardness testing machine under 10Kgf load. Testing was done from centre of weld zone towards the both side of joint. Prior to testing, samples were mechanically polished. Results showed that for all the cases of TIG welding, hardness value of base metal showed higher than that at welding zone. Hardness value starts decreasing towards the HAZ and increases in the welding region. Base metal had a hardness value of 103.65(HV).

Fig.6 Shows the average hardness values at the different current condition. There is no consistent rise or fall in hardness value observed with increase in current value. The current value of 70A and 80A shows negligible difference in hardness, whereas increase in hardness value with increase in current were observed at 75A, 85A and 90A. Current value of 70A, 80A and 90A shows higher values of hardness, whereas current 75A and 85A shows lower hardness value with a maximum hardness value of 55.4(HV) at 90A and minimum hardness value of 50.9(HV) observed at current value of 75A. The hardest and softest samples had a difference in hardness of about 4.5(HV).

**Table 7:** Hardness and welding Dilution of the samples

Current Value(I)Amperes	Hardness Value	Dilution level of Aluminium, %	Dilution level of Magnesium, %	Dilution level of Silicon, %
70	54.3	27.77	38.26	37.18
75	50.9	32.78	56	70.59
80	54	30.58	43.85	53.96
85	52.8	35.08	51.54	56.23
90	55.4	36.72	61.43	73.08

**Fig.7:** Correlating hardness and welding dilution levels of the samples

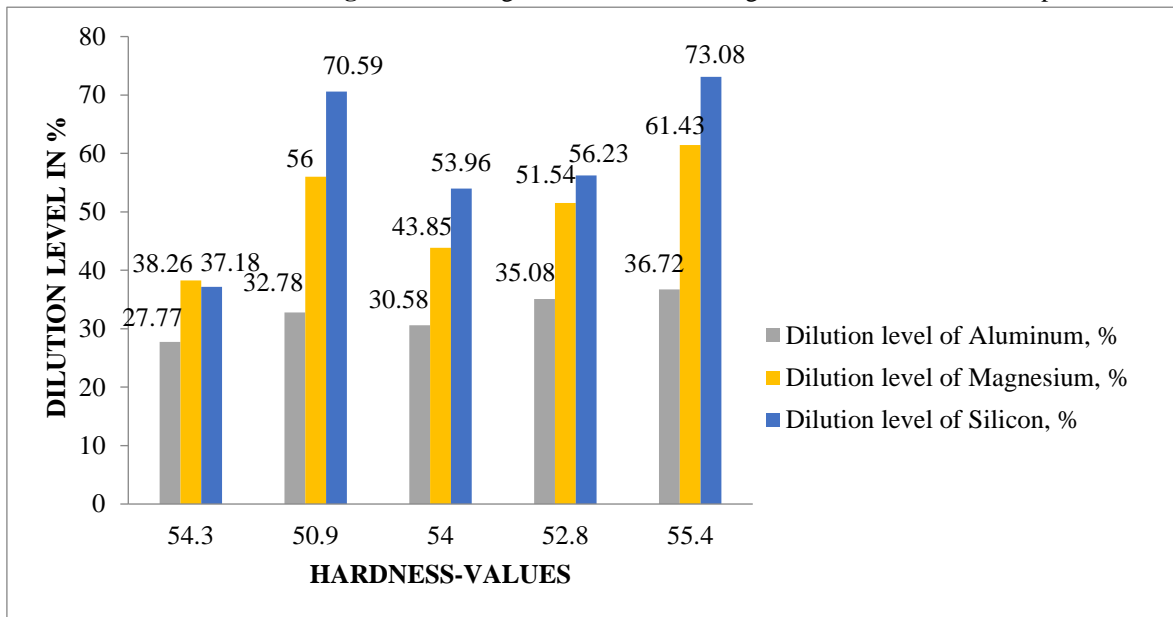


Figure 7 shows Correlation of hardness and dilution values with respect to varying current. The trend of variation in dilution with increase in current is similar. It is seen from the figure that dilution level in Al ,Mg and Si increases with increase in current value up to 75A and decrease in value of dilution is observed at current value 80A, but further increase in current value increase in dilution is observed.

It is also observed that Al shows lower values of dilution and silicon shows higher values of dilution at all the current values, whereas dilution of Mg lies between Al and Si. Except at the hardness value of 54.3(HV) at all other hardness value Si shows maximum dilution level, whereas dilution level of Mg is in between. Comparing between Si and Al, maximum difference of 37.81% in dilution observed at lowest value of hardness 50.9(HV). Where as maximum difference of 24.71% between Al and Mg is observed at highest value of hardness 54.4(HV).

It is seen from the table 7 that by looking at the relationship between current and dilution, the sample welded with 70A had the lowest value of dilution while the highest dilution was obtained for the sample welded using 90A.

To correlate between hardness and dilution with current, it is observed that maximum value of dilution and hardness is observed at highest value of current 90A.

4.3 Effect of weld pool flow on Dilution level

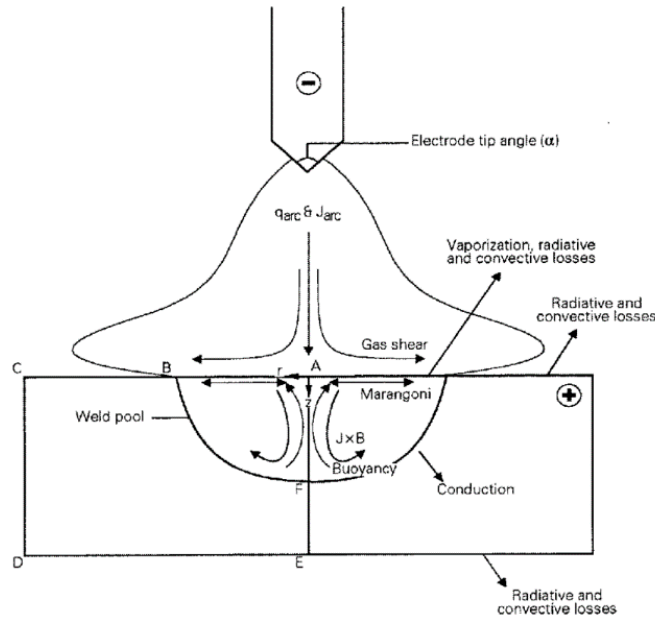


Fig. 8: The shape and fluid flow pattern of the weld pool

The fluid flow in the weld pool is subjected to the interaction among several forces including droplet impinging force, electromagnetic force, buoyancy force due to temperature and silicon gradient and surface tension. Electromagnetic force produces a flow radially inward and downward near the centre of the weld pool. Buoyancy force results from the difference in temperature and concentration in the weld pool. Because the weld pool is small and the hot fluid is at the top of the pool, the buoyancy force due to temperature gradient is expected to be small, as compared to the electromagnetic force. The weld pool surface can be considered to be flat when the arc current is below 200A. Droplet impinging momentum is considered to play an important role in determining the fluid flow in the weld pool. At the instant when the droplet impact the weld pool surface, the droplet tends to push its surrounding fluid away and sink to the bottom of the weld pool. The phenomenon are similar to those of a rock falling in to a pond. Surface tension force, a function of temperature and silicon concentration is expected to be very important in GTAW.

The shape and fluid flow pattern of the weld pool is as shown in the figure 8. The fluid flow pattern in the weld pool is generally downward along the centre of the weld pool and then upward along the liquid and solid interface, creating a counter clockwise vortex. The maximum flow velocity in the weld pool is approximately 0.08m/s. Note that the Reynolds number, based on the size of the weld pool and maximum flow velocity is approximately 100, which indicates that the fluid flow in the weld pool is laminar.

Table 8: Weld pool effect on dilution

Sl.No.	Current Value (I) Amperes	Dilution Si %
1	70	37.18
2	75	70.59
3	80	53.96
4	85	56.20
5	90	73.08

From the above table it is seen that since Si being an active element, increased dilution level is observed due to weld pool flow at higher current of 90A.

Effect of weld pool flow on dilution level as a result, the dilution decreases. Conversely, welds made with a fixed feed rate exhibit an increase in dilution with increasing arc power. In this case, the  $A_{fm}$  term is essentially constant, but the increase in arc power increases the amount of base metal melted, thus leading to an increase in the dilution level.

5. Conclusions

5.1 Observing the dilution level values of aluminium in Al 6061 with 4043 as filler alloy by varying the current, the dilution level at the top is low compared to dilution level at the middle and it is moderate at the bottom.

5.2 Due to active element of silicon in the filler alloy there is a reverse marangoni flow takes place so that there is a high percentage level in dilution of silicon at the middle and moderately at top and bottom. The reverse marangoni convection direction from outward to inward in Si element. This created a narrower deeper weld pool for exactly the same welding conditions of varying currents. By decreasing the current the dilution level decreases.

- 5.3 The magnesium element is very much stable due to presence of Silicon element in Al6061 material, dilution level is moderate in top and bottom level and very good at the middle and hence good weld pool at the center.
- 5.4 The results of SEM and EDS indicated that Si particles were involved and distributed dispersed in the weld bead because of the inwards direction of the molten metal flowed and the Silicon content in the centre of the weld was bigger than that in the edge of the weld.
- 5.5 Greater hardness and dilution can be observed by increasing the current.
- 5.6 Surface tension is the major driving force contributing to the weld pool fluid flow, mixing and weld penetration in GTAW.
- 5.7 A higher silicon concentration in droplets produces an inward flow at the surface of the weld pool, which carries arc energy downward and leads to deep weld penetration and good weld mixing.
- 5.8 TIG welding can be used to weld thicker as well as thinner materials. The parameter of current makes it easily controllable. As the current increases the grains formed are smaller in size, but optimization is required depending upon the thickness of the base metal used. The presence of a gas also makes it more susceptible to development of porosity in the resultant material.

## 6. Acknowledgements

The present work was supported by Department of Industrial Engineering and Management, Bangalore Institute of Technology, Bengaluru, India.

## References

1. Cary HB (1989) Modern welding technology. Prentice-Hall, Upper Saddle River, NJ
2. Metzger GE (1967) Some mechanical properties of welds in 6061 aluminum alloy sheet. *Welding J* 46(10):457s-469s
3. Simpson RP (1997) Controlled weld pool solidification and resultant properties with Yttrium inoculation of Ti-6Al-6V-2Sn welds. *Welding J* 56(3):67s-72s
4. Kou S, Le Y (1986) Nucleation mechanism and grain refining of weld metal. *Welding J* 65(4):65-70
5. Tsang TS, Savage D (1971) The effect of arc oscillation in either transverse or longitudinal direction has beneficial effect on the fusion zone microstructure and tends to reduce sensitivity to hot cracking. *Welding J* 50(11):777-786
6. Madusudhan Reddy G, Gokhale AA, Prasad Rao K (1997) Weld microstructure refinement in a 1441 grade Al-Lithium alloy. *J Mater Sci* 32:4117-4121, DOI 10.1023/A:1018662126268
7. Kramer LS, Pickens JR (1992) Microstructure and properties of a welded Al-Cu-Li alloy. *Welding J* 71(4):115s-121s
8. Banovic SW, Dupont JN, Marde AK (2002) Dilution and micro segregation in dissimilar metal welds between super austenitic steels and nickel-base alloys. *Sci Technol Weld Join* 7(6):374-383, DOI 10.1179/136217102225006804
9. S.W. Banovic, J.N. DuPont and A.R. Marder (2001) Dilution Control in Gas-Tungsten-Arc Welds Involving Super austenitic Stainless Steels and Nickel-Based Alloys, *Journal of Metallurgical and Materials Transactions B*, Volume 32B, P1171-1176.
10. A. Kumar, S. Sundarajan (2009), Effect of welding parameters on mechanical properties and optimization of pulsed TIG welding of Al-Mg-Si alloy, *Int. J. Adv. Manuf. Technol* 42:118-125.
11. Shanping Lu, Hidetoshi Fujii et al., (2002), Weld Penetration and Marangoni Convection with Oxide Fluxes in GTA Welding, *Materials Transactions*, Vol. 43, No. 11, pp 2926-2931.
12. Zhaodong Zhang, Liming Liu et al., AC TIG welding with single-component oxide activating flux for AZ31B magnesium alloys, *J Mater Sci* 43:1382-1388
13. L. Liu & Sun (2008), Study of flux assisted TIG welding of magnesium alloy with SiC particles in flux, *Materials Research Innovations*, Vol 12, No. 1, pp 47-51
14. T. Sandor, C. Mekler, J. Dobranszky, G. Kaptay (2013), An Improved Theoretical Model for A-TIG Welding Based On Surface Phase Transition and Reversed Marangoni Flow, *Metallurgical and Materials Transactions A*, Volume 44A, pp 351-361.
15. J. Paulo Davin, Aveiro, Portugal, prakriti kumar ghosh, pulse current gas metal arc welding, *Materials Forming, Machining and Tribology*, Springer Nature Singapore Pte Ltd. 2017, ISBN 978-981-10-3556-2 ISBN 978-981-10-3557-9 (eBook) DOI 10.1007/978-981-10-3557-9
16. Hein Zaw Oo, BSrikarun, and P. Muangjunburee "Correlating Hardness and Welding Dilution with the Abrasion Mass Loss of Hardfacings welded with Different currents and Polarities" *Springer Science+Business Media, LLC, Metallurgist*, Vol. 61, Nos. 11-12, March 2018, pp 1033-1037.
17. Y. WANG and H.L. TSAI "Effects of Surface Active Elements on Weld Pool Fluid Flow and weld Penetration in Gas metal arc welding." *Metallurgical and materials transaction B*, Volume 32B, June 2001-P501-514